Pacific origin of the abrupt increase in Indian Ocean heat content during the warming hiatus. [and Supplementary Information]

nature geoscience

SUPPLEMENTARY INFORMATION

DOI: 10.1038/NGEO2438

Pacific origin of the abrupt increase in Indian Ocean heat content during the warming hiatus

Sang-Ki Lee[1,2,*], Wonsun Park[3], Molly O. Baringer[2], Arnold L. Gordon[4], Bruce Huber[4] and Yanyun Liu[1,2]

[1]Cooperative Institute for Marine and Atmospheric Studies, University of Miami, Miami, Florida 33149, USA
[2]Atlantic Oceanographic and Meteorological Laboratory, NOAA, Miami, Florida 33149, USA
[3]GEOMAR Helmholtz Centre for Ocean Research Kiel, D-24105 Kiel, Germany
[4]Lamont-Doherty Earth Observatory, Earth Institute at Columbia University, Palisades, New York 10964, USA

Table of Contents

DOI: 10.1038/NGEO2438

S.I.1. Discussion on the World Ocean Atlas 2013

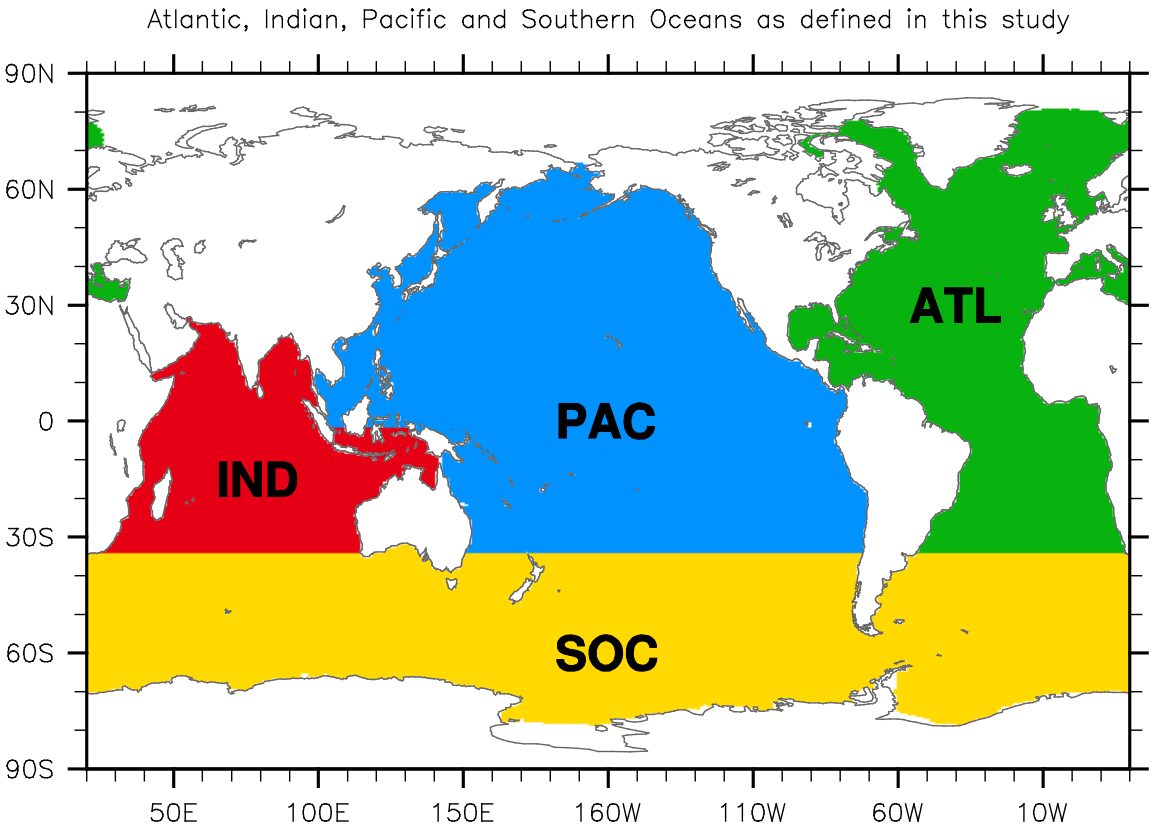

Figure S1. Four major ocean basins defined in this study. The Atlantic Ocean (ATL) includes the Mediterranean Sea and the Labrador Sea. The Southern Ocean (SOC) is directly connected to the Atlantic, Pacific and Indian Oceans at 34°S. The Indian Ocean (IND) and the Pacific Ocean (PAC) are directly connected via the Indonesian passages across 1.6°S. The contribution of the Arctic Sea on the global ocean heat change is very small thus not discussed in this study.

The World Ocean Atlas 2013 (WOA13)[1] was used to compute OHC_{700} for the global ocean, and for the Atlantic, Pacific, Indian and Southern Oceans (Fig. S1). The rates of OHC_{700} change for the global ocean, and for the Indian, Pacific, Atlantic and Southern Oceans, computed from WOA13, are shown in Table S1.

Table S1. Rates of OHC_{700} change for the global ocean and the four major ocean basins. The rates of OHC_{700} change for the global ocean, and for the Indian, Pacific, Atlantic and Southern Oceans, derived from WOA13, are shown for the periods of 1971-2000 and 2003-2012. The unit is 10^{22} J per decade.

Periods	Global Ocean	Indian Ocean	Pacific Ocean	Atlantic Ocean	Southern Ocean
1971-2000	2.8	-0.2	0.9	1.3	0.6
2003-2012	2.9	2.1	-0.4	-0.3	1.5

For the ocean heat content changes below 700 m, there is no reliable in-situ global deep ocean data before the Argo observations whose spatial coverage over the global ocean reached a mature state only around 2004-2005. Since there is no reliable global deep ocean observation data for the study period (1971-2012), the ocean heat content changes below 700 m were not explored in this study.

It should be also noted that the OHC_{700} derived from WOA13 increased sharply during 2001-2003 in all ocean basins including the Atlantic and Southern Oceans (Figs. 1 and S2). Previous studies have suggested that the changes in the historical observation network from a ship-based system to Argo floats introduced an artificial jump in OHC_{700} during the initiation of the global Argo array (2001-2003)[2,3,4]. Therefore, the OHC_{700} changes derived from WOA13 during 2001-2003 were not used in this study.

S.I.2. Recent OHC_{700} changes and heat budget for the Atlantic and Southern Oceans

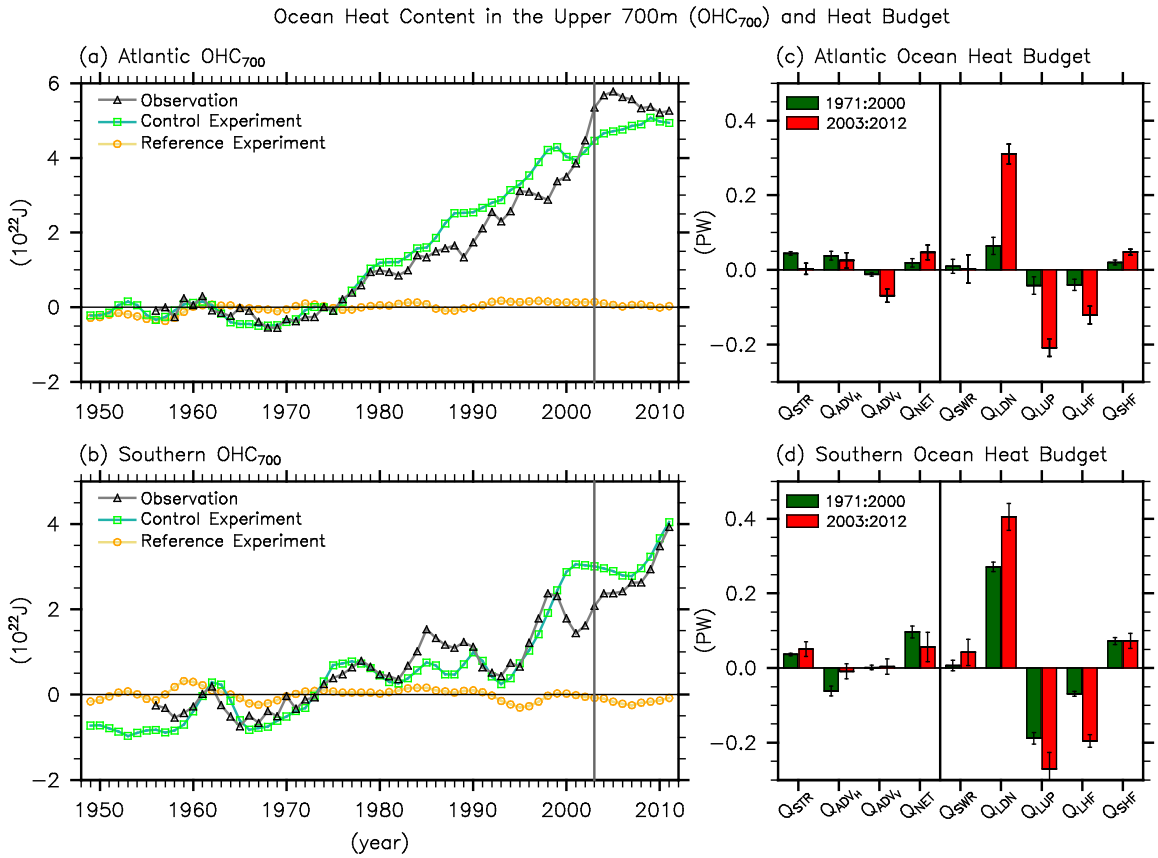

Figure S2. OHC_{700} and heat budget for the Atlantic and Southern Oceans. Time series of OHC_{700} for (a) the Atlantic and (b) Southern Oceans derived from the control and reference experiments and observations[12] are shown. The heat budget terms, namely the storage rate (Q_{STR}), horizontal and vertical advections (Q_{ADV_H} and Q_{ADV_V}), net surface heat flux (Q_{NET}), shortwave radiation (Q_{SWR}), downward and upward longwave radiations (Q_{LDN} and Q_{LUP}), latent heat flux (Q_{LHF}) and sensible heat flux (Q_{SHF}), for (c) the Atlantic and (d) Southern Oceans derived from the control experiment relative to the reference experiment are averaged for the 1971-2000 (green bars) and 2003-2012 periods (red bars). The error bars show the 90 % confidence levels derived from the six-member ensemble runs.

Overall, the control experiment reasonably well captured the observational estimates of OHC_{700} changes in the Atlantic and Southern Oceans since the 1970s (Figs. S2a and S2b). As discussed in S.I.1, however, the OHC_{700} derived from WOA13 increased sharply during 2001-2003 in the Atlantic and Southern Oceans likely due to the changes in historical observation network from a ship-based system to Argo floats[2,3,4]. The simulated OHC_{700} from the control experiments does not show such a sharp increase during this period either in the Atlantic Ocean or in the Southern Ocean.

DOI: 10.1038/NGEO2438

In the Atlantic Ocean, the surface heat uptake increased considerably during 2003-2012 in comparison to the earlier period of 1971-2000. However, a large portion of the anomalous surface heat uptake was transported to the deeper ocean below 700 m ($Q_{ADV_v} < 0$), consistent with previous studies[5,6]; thus, the OHC_{700} did not increase much during 2003-2012 (Figs. S2a and S2c).

In the Southern Ocean, the surface heat uptake reduced somewhat during 2003-2012 in comparison to the earlier period of 1971-2000. Nevertheless, the OHC_{700} did increase during 2003-2012 with a slightly higher rate than that during 1971-2000 (Figs. S2b and S2d) mainly because the southward heat transport into the Southern Ocean across 34° (mainly from the Indian Ocean; see Table S6) increased during 2003-2012 in comparison to the earlier period of 1971-2000.

Additionally, there was no significant transport of heat to the deeper Southern Ocean disagreeing with previous studies[5,6]. However, since there is no reliable in-situ deep ocean data in the Southern Ocean for the study period (1971-2012) and the current state-of-the-art ocean-sea ice models in general have difficulties in reproducing the climatology in the Southern Ocean[7], the heat budget analysis result for the Southern Ocean and its implication for the deeper Southern Ocean should be interpreted with caution.

S.I.3. Discussion on the bias-corrected 20CR surface flux fields

In order to minimize potential biases in the 20CR surface flux fields (see ref 8), the monthly climatologies and high-frequency variability of the 20CR surface flux fields were corrected using the surface flux fields derived from the common ocean-ice reference experiments version 2 (CORE2; ref 9), which is a global surface flux data set corrected by using available observations.

We first constructed a set of monthly surface flux climatologies using the 20CR surface flux variables for 1984-2006, and another set of monthly surface flux climatologies using the CORE2 surface flux variables for the same period. Then, the differences between the two sets of climatologies (i.e., CORE2 - 20CR) were added to the 20CR surface forcing fields.

After correcting the monthly climatologies in the 20CR surface flux variables, a 5-day high-pass filter was applied to the CORE2 surface flux fields to obtain high-frequency variability in the CORE2 surface flux fields. Similarly, a 5-day low-pass filter was applied to the above processed 20CR surface forcing fields to remove high-frequency variability. Then, for each model year (from 1948 to 2012), the high-pass filtered CORE2 surface flux fields for a randomly selected year during 1984-2006 were added to the low-pass filtered 20CR surface flux fields to construct the bias-corrected 20CR surface flux fields.

S.I.4. Discussion on the spin-up run

It is a common practice to spin up an ocean model with a seasonally varying climatological surface flux data set. However, recent studies have suggested that weather noise (linked to winter storms for example) and interannual-frequency surface forcing (linked to the North Atlantic Oscillation for example) are also important in shaping the mean state of the global ocean[10]. The spin-up method with randomly selected forcing years used in this study[11] (Method) conserves the

total variance of the surface flux fields without introducing spurious long-term variability. Therefore, it is an effective way to spin up any ocean or ocean-sea ice coupled models.

S.I.5. Discussion on the heat budget analysis

The heat budgets summarized in Figs. 1 and S2 were obtained by first integrating the heat budget terms derived from the control experiment for the global ocean and for the individual major ocean basins. The spatially integrated heat budget terms for the global ocean and for the individual ocean basins were then averaged for the 1971-2000 and for 2003-2012 periods. The same procedure was used to compute the corresponding heat budget terms from the reference experiment, which were later subtracted from those derived from the control experiment. Therefore, the heat budget terms shown in Figs. 1 and S2 are the time-averaged values for the 1971-2000 and 2003-2012 periods in the control experiment relative to the reference experiment.

The heat budget values obtained from the control experiment for 1971-2000 and 2003-2012, the 30-year mean and 10-year mean of the reference experiment, and the differences (control experiment for 1971-2000 minus 30-year mean of the reference experiment; control experiment for 2003-2012 minus 10-year mean of the reference experiment) are summarized in Table S2, S3, S4, S5 and S6 for the global ocean and for the Indian, Pacific, Atlantic and Southern Oceans, respectively. The heat budget values for the control experiment are based on the 6-member ensemble averages. For the reference experiment, the 6-member ensemble averages of the 424-453, 524-553, 624-653, 724-753, 824-853, and 924-953 model years were used to obtain the 30-year mean heat budget values. Similarly, the 6-member ensemble averages of the 456-465, 556-565, 656-665, 756-765, 856-865, and 956-965 model years were used to obtain the 10-year mean heat budget values.

Table S2. **Heat budget for the global ocean in the upper 700 m**. The heat budget terms for the global ocean in the upper 700 m derived from the control experiment for 1971-2000 and 2003-2012, the 30-year mean and 10-year mean of the reference experiment and the differences (control experiment for 1971-2000 minus 30-year mean of the reference experiment; control experiment for 2003-2012 minus 10-year mean of the reference experiment) are shown. The unit is PW.

Heat budget terms	1971-2000			2003-2012		
	Control	Reference	Control – Reference	Control	Reference	Control – Reference
Q_{STR}	0.10	0.00	**0.10**	0.12	0.01	**0.11**
Q_{NET}	0.12	-0.02	**0.15**	0.19	-0.03	**0.23**
Q_{SWR}	59.51	59.34	**0.17**	59.46	59.36	**0.10**
Q_{LHF}	-34.10	-33.75	**-0.35**	-34.48	-33.76	**-0.72**
Q_{SHF}	-5.41	-5.57	**0.16**	-5.30	-5.58	**0.28**
Q_{LDN}	123.34	122.75	**0.58**	124.17	122.72	**1.45**
Q_{LUP}	-143.11	-142.69	**-0.42**	-143.56	-142.68	**-0.88**
Q_{ADV_v}	-0.02	0.02	**-0.04**	-0.08	0.04	**-0.12**

DOI: 10.1038/NGEO2438

Table S3. Heat budget for the Indian Ocean in the upper 700 m. Same as Table S2, except for the Indian Ocean.

Heat budget terms	1971-2000			2003-2012		
	Control	Reference	Control – Reference	Control	Reference	Control – Reference
Q_{STR}	0.00	0.00	**0.00**	0.07	0.00	**0.07**
Q_{NET}	0.13	0.11	**0.02**	0.11	0.12	**-0.01**
Q_{SWR}	9.55	9.49	**0.06**	9.57	9.51	**0.06**
Q_{LHF}	-5.99	-5.88	**-0.11**	-6.10	-5.88	**-0.22**
Q_{SHF}	-0.64	-0.68	**0.03**	-0.63	-0.68	**0.05**
Q_{LDN}	17.89	17.81	**0.07**	18.01	17.81	**0.12**
Q_{LUP}	20.68	-20.65	**-0.03**	-20.74	-20.65	**-0.09**
Q_{ADV_H} (SOC to IND)	-1.11	-1.12	**0.01**	-1.18	-1.11	**-0.07**
Q_{ADV_H} (PAC to IND)	0.96	0.97	**-0.01**	1.14	0.95	**0.19**
Q_{ADV_V}	0.02	0.04	**-0.01**	0.00	0.04	**-0.04**

Table S4. Heat budget for the Pacific Ocean in the upper 700 m. Same as Table S2, except for the Pacific Ocean.

Heat budget terms	1971-2000			2003-2012		
	Control	Reference	Control – Reference	Control	Reference	Control – Reference
Q_{STR}	0.02	0.00	**0.02**	-0.02	0.00	**-0.02**
Q_{NET}	0.82	0.81	**0.02**	0.93	0.79	**0.13**
Q_{SWR}	26.32	26.25	**0.08**	26.22	26.26	**-0.04**
Q_{LHF}	-15.63	-15.50	**-0.13**	-15.69	-15.52	**-0.18**
Q_{SHF}	-2.08	-2.12	**0.04**	-2.01	-2.12	**0.11**
Q_{LDN}	52.31	52.21	**0.10**	52.57	52.21	**0.36**
Q_{LUP}	-60.08	-60.01	**-0.07**	-60.14	-60.01	**-0.13**
Q_{ADV_H} (SOC to PAC)	0.24	0.23	**0.01**	0.27	0.22	**0.06**
Q_{ADV_H} (IND to PAC)	-0.96	-0.97	**0.01**	-1.14	-0.95	**-0.19**
Q_{ADV_V}	-0.09	-0.07	**-0.02**	-0.08	-0.06	**-0.02**

Table S5. Heat budget for the Atlantic Ocean in the upper 700 m. Same as Table S2, except for the Atlantic Ocean.

Heat budget terms	1971-2000			2003-2012		
	Control	Reference	Control – Reference	Control	Reference	Control – Reference
Q_{STR}	0.05	0.00	**0.04**	0.00	0.00	**0.00**
Q_{NET}	-0.31	-0.33	**0.02**	-0.29	-0.34	**0.05**
Q_{SWR}	12.72	12.71	**0.01**	12.72	12.72	**0.00**
Q_{LHF}	-7.57	-7.53	**-0.04**	-7.66	-7.54	**-0.12**
Q_{SHF}	-1.176	-1.20	**0.02**	-1.15	-1.20	**0.05**
Q_{LDN}	25.42	25.36	**0.06**	25.67	25.36	**0.31**
Q_{LUP}	-29.65	-29.60	**-0.04**	-29.81	-29.61	**-0.22**
Q_{ADV_H} (SOC to ATL)	0.65	0.61	**0.04**	0.63	0.61	**0.03**
Q_{ADV_V}	-0.29	-0.28	**-0.01**	-0.34	-0.27	**-0.07**

Table S6. Heat budget for the Southern Ocean in the upper 700 m. Same as Table S2, except for the Southern Ocean.

Heat budget terms	1971-2000			2003-2012		
	Control	Reference	Control – Reference	Control	Reference	Control – Reference
Q_{STR}	0.04	0.00	**0.04**	0.06	0.00	**0.05**
Q_{NET}	-0.46	-0.56	**0.10**	-0.50	-0.56	**0.06**
Q_{SWR}	10.54	10.54	**0.01**	10.58	10.54	**0.04**
Q_{LHF}	-4.66	-4.59	**-0.07**	-4.78	-4.58	**-0.20**
Q_{SHF}	-1.38	-1.45	**0.07**	-1.38	-1.45	**0.07**
Q_{LDN}	26.20	25.93	**0.27**	26.33	25.92	**0.40**
Q_{LUP}	-30.91	-30.72	**-0.19**	-30.99	-30.72	**-0.27**
Q_{ADV_H} (ATL to SOC)	-0.65	-0.61	**-0.04**	-0.63	-0.61	**-0.03**
Q_{ADV_H} (IND to SOC)	1.11	1.12	**-0.01**	1.18	1.11	**0.07**
Q_{ADV_H} (PAC to SOC)	-0.24	-0.23	**-0.01**	-0.27	-0.22	**-0.06**
Q_{ADV_V}	0.28	0.28	**0.00**	0.29	0.28	**0.00**

As shown in Tables S3 and S4, the inter-ocean heat transport from the Pacific to the Indian Ocean via the Indonesian passages greatly increased during 2003-2012 (~ 0.19 PW). During the same period, the southward heat transport from the Indian Ocean to the Southern Ocean across 34ºS increased (~ -0.07 PW; the negative indicates transport from the Pacific Ocean to the Indian Ocean) and thus slightly decreased the heat gain from the Pacific Ocean. In the Pacific Ocean, the increased inter-ocean heat transport from the Pacific to the Indian Ocean (~ -0.19 PW; the negative indicates transport from the Pacific Ocean to the Indian Ocean) was somewhat compensated by the increased northward heat transport from the Southern Ocean to the Pacific Ocean across 34ºS (~ 0.06 PW).

S.I.6. Discussion on the three sensitivity experiments

Additional sensitivity experiments (Methods) were carried out to further understand the relative importance of wind forcing from the different ocean basins in driving the ITF variability. Using real-time surface winds *inside* the Pacific Ocean and climatological winds *outside* of the Pacific Ocean (EXP_PAC), the abrupt increase of the Indian OHC_{700} during the 2000s was successfully simulated, whereas ensemble runs forced by real-time surface winds *inside* the Southern Ocean and climatological surface winds *outside* of the Southern Ocean (EXP_SOC) almost completely failed to reproduce the Indian OHC_{700} increase in the 2000s (Fig. 4a).

Using real-time surface winds *inside* the Indian Ocean and climatological surface winds *outside* of the Indian Ocean (EXP_IND), the ensemble runs captured the Indian OHC_{700} increase, although only a small fraction of it (Fig. 4a). In both EXP_PAC and EXP_IND, the heat budget also indicates that the inter-ocean heat transport carried by the ITF increased during 2003-2012, albeit more so in EXP_PAC than in EXP_IND (Fig. 4c). Therefore, these sensitivity experiments confirm that the anomalous surface wind fields in the Pacific and Indian Oceans are the key to increasing the ITF heat transport in the control experiment during 2003-2012.

References

1. Levitus, S., Antonov, J. I., Boyer, T. P., Locarnini, R. A., Garcia, H. E. & Mishonov A. V. Global ocean heat content 1955–2008 in light of recently revealed instrumentation problems. *Geophys. Res. Lett*. **36,** L07608 (2009).

DOI: 10.1038/NGEO2438

2. Cheng, L. & Zhu, J. Artifacts in variations of ocean heat content induced by the observation system changes. *Geophys. Res. Lett*. **41**, 7276–7283 (2014).
3. Lyman, J. M. & Johnson, G. C. Estimating global ocean heat content changes in the upper 1800 m since 1950 and the influence of climatology choice. *J. Clim*. **27**, 1945–1957 (2014).
4. Balmaseda, M. A., Trenberth, K. E., & Källén, E. Distinctive climate signals in reanalysis of global ocean heat content. *Geophys. Res. Lett.* **40**, 1754–1759 (2013).
5. Chen, X. & Tung, K.-K. Varying planetary heat sink led to global-warming slowdown and acceleration. *Science* **345**, 897-903 (2014).
6. Drijfhout, S. S., Blaker, A. T., Josey, S. A., Nurser, J. G., Sinha, B. & Balmaseda, M. A. Surface warming hiatus caused by increased heat uptake across multiple ocean basins. *Geophys. Res. Lett*. **41**, 7868–7874 (2014).
7. Weijer, W., Sloyan, B. M., Maltrud, M. E., Jeffery, N., Hecht, M. W., Hartin, C. A., van Sebille, E., Wainer, I. & Landrum, L. The Southern Ocean and its climate in CCSM4. *J. Clim*. **25**, 2652–2675 (2012).
8. Krüger O., Schenk F., Feser F. & Weisse R. Inconsistencies between long-term trends in storminess derived from the 20CR reanalysis and observations. *J. Clim*. 26, 868-874 (2013).
9. Large W. G. &Yeager, S. G. The global climatology of an interannually varying air–sea flux data set. *Clim. Dyn*. **33**, 341-364 (2009).
10. Kirtman, B. P., Bitz, C., Bryan, F., Collins, W., Dennis, J., Hearn, N., Kinter III, J. L., Loft, R., Rousset, C., Siqueira, L., Stan, C., Tomas, R. & Vertenstein, M. Impact of ocean model resolution on CCSM climate simulations. *Clim. Dyn*. **39**, 1303-1328 (2012).
11. Lee, S.-K., Park, W., van Sebille, E., Baringer, M. O., Wang, C., Enfield, D. B., Yeager, S. & Kirtman, B. P. What caused the significant increase in Atlantic Ocean heat content since the mid-20th century? *Geophys. Res. Lett*. **38**, L17607 (2011).